Available online at www.sciencedirect.com
ScienceDirect
Journal of Nuclear Materials 367–370 (2007) 202–207
journal of nuclear materials
www.elsevier.com/locate/jnucmat

Microstructural development of a heavily neutron-irradiated ODS ferritic steel (MA957) at elevated temperature

S. Yamashita [a,*], N. Akasaka [a], S. Ukai [a], S. Ohnuki [b]

[a] *Oarai Research and Development Center, Japan Atomic Energy Agency (JAEA), 4002 Narita-cho, Oarai-machi, Ibaraki 311-1393, Japan*
[b] *Graduate School of Engineering, Hokkaido University, N-13, W-8, Sapporo 060-8628, Japan*

Abstract

Microstructural observation was performed on a neutron-irradiated oxide dispersion strengthened (ODS) ferritic steel with emphasis on oxide behavior, including phase stability under irradiation at elevated temperature (~973 K). Transmission electron microscopy observation of the Y–Ti complex oxide particles showed they were fine (~40 nm) whereas the Ti-oxide particles were relatively coarse (~300 nm). Dispersion parameters of oxide particles, such as mean size and number density, changed due to irradiation. This implies recoil resolution of the oxide particles. When irradiated at 973 K, some Y–Ti complex oxides survived and interacted with the dislocation structures, which delayed the dislocation recovery and stabilized the elongated grain structure. It is considered that oxide particles could be effective pinning points of dislocations in motion under irradiation to a dose of ~100 dpa.

1. Introduction

To achieve high thermal efficiency for solid breeder blankets of fusion reactors or fuel pins in liquid metal fast fission reactors, candidate structural materials must have good tolerance for irradiation-induced void swelling and for irradiation-enhanced creep at elevated temperature.

For the last few decades, oxide dispersion strengthened (ODS) steels which promise better high temperature creep properties than conventional ferritic/martensitic steels and greater dimensional stability than austenitic steels have been vigorously studied for applications in fast reactors [1–3]. Based on the results of extensive research and development (R&D), two ODS alloys for cladding tubes with base compositions Fe–0.12C–9Cr–2W–0.2Ti–0.35Y_2O_3 and Fe–12Cr–2W–0.3Ti–0.24Y_2O_3 have been fabricated; these alloys were developed to reduce the anisotropy of mechanical properties attributed to their processing [4,5]. Both have a more desirable grain morphology, i.e. equiaxial grains, obtained by utilizing phase transformation or recrystallization, respectively. Tubes made of these ODS steels have been irradiated to a maximum dose of ~15 dpa in the experimental fast reactor JOYO and have been verified to be very irradiation tolerant materials [6].

Among current R&D issues for ODS steels, extending the available range of irradiation data is as important as developing advanced ODS steels

* Corresponding author. Tel.: +81 29 267 4141; fax: +81 29 266 3713.
E-mail address: yamashita.shinichiro@jaea.go.jp (S. Yamashita).

0022-3115/$ - see front matter © 2007 Elsevier B.V. All rights reserved.
doi:10.1016/j.jnucmat.2007.03.145

by composition/processing optimization. Thus, the present study focused on the microstructural evolution of one ODS ferritic steel (MA957) that was irradiated to a dose of ~100 dpa at a temperature from 775 to 973 K, conditions at which the performance of ODS steels is generally thought to be degraded. This extended the high temperature side of the irradiation data field. Since MA957 has been investigated from various viewpoints [7–12], special emphasis in this study was on oxide behavior, including phase stability under irradiation at elevated temperatures (~973 K).

2. Experimental procedure

The material used in this investigation was a commercially produced ODS steel, INCO MA957, in which yttrium oxide (Y_2O_3) particles were dispersed. The analyzed composition of the MA957 was Fe–13.9Cr–1.0Ti–0.31Mo–0.27Y_2O_3–0.18O (mass%). This oxygen content was differentiated from the oxygen component of Y_2O_3.

The MA957 samples, in sheet form, were neutron-irradiated in the core materials irradiation rig (CMIR) through successive irradiation campaigns in JOYO. The irradiated MA957 sheets were unloaded at the end of the third, fourth, and fifth irradiation cycles, coupons were cut from them and then the sheets were reloaded to continue irradiation. Details of the irradiation conditions are shown in Table 1.

Table 1
Irradiation conditions of INCO MA957

CMIR campaign no.	~2	3	4	5	Remark temperature (K)
Cumulative time (h)	9880	14 520	18 740	23 540	
Cumulative dose (dpa)	44.5	65.0*	84.0	101.0*	775
	52.5	76.5*	99.0*	–	862
	53.0	77.5*	100.5*	–	982

* Microstructural observations were done for the specimens irradiated under the conditions indicated by the asterisks.

Samples for transmission electron microscopy (TEM) were prepared from the irradiated MA957 sheets as follows. The coupons that were cut from the irradiated sheets were mechanically thinned to ⩽0.15 mm. The thinned coupons were punched to get 3 mm discs. These discs were electro-polished at 288 K and 90–100 mA with an electrolytic solution of CH_3COOH:$HClO_4$ in the ratio 19:1.

Microstructural observations used a conventional TEM (JEM-4000FX) operated at 400 kV and/or a high resolution TEM (JEM-2010F) at 200 kV. Microchemical analyses were performed utilizing an energy dispersive spectrum (EDS) device on the electron microscope.

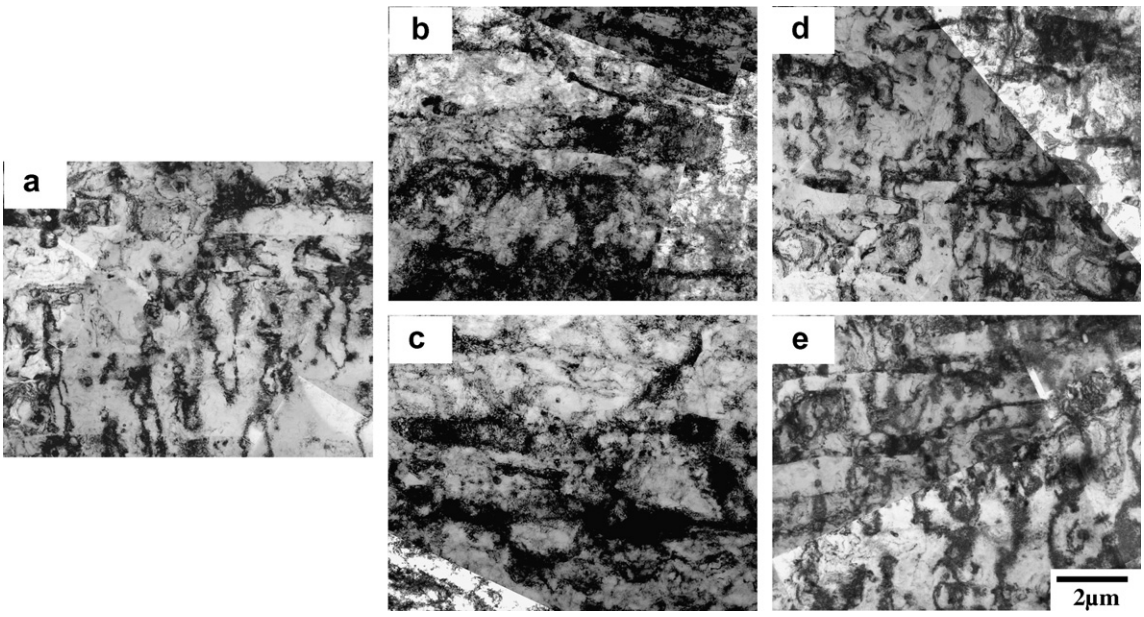

Fig. 1. Bright field TEM micrographs of MA957: (a) as-received, irradiated at 775 K (b) to 65.0 dpa and (d) to 101.0 dpa, and irradiated at 982 K (c) to 77.5 dpa and (e) to 100.5 dpa.

3. Results

TEM micrographs of MA957 specimens before and after irradiation are shown in Fig. 1(a)–(e). Prior to irradiation (Fig. 1(a)), MA957 had elongated ferritic grains which had developed during the fabrication of the consolidated bar from mechanical alloying (MA) powder. When Fig. 1(a), (b) and (d) are compared, the elongated ferritic grains were seen not to change to any extent by irradiation at 775 K up to a dose of 104 dpa. Comparison of Fig. 1(a), (c) and (e) show little microstructural evolution of MA957 even at 982 K.

The micrographs in Fig. 2 show small cavities observed in the ferritic matrix before and after irradiation. Most cavities prior to irradiation (Fig. 2(a)) were concentrated at the precipitate–matrix interface. Some cavities were also found in the matrix. Based on past experiences with ODS steel fabrication, these cavities were deduced to be Ar gas bubbles trapped during fabrication. Fig. 2(b) shows that after irradiation at 775 K cavities were concentrated

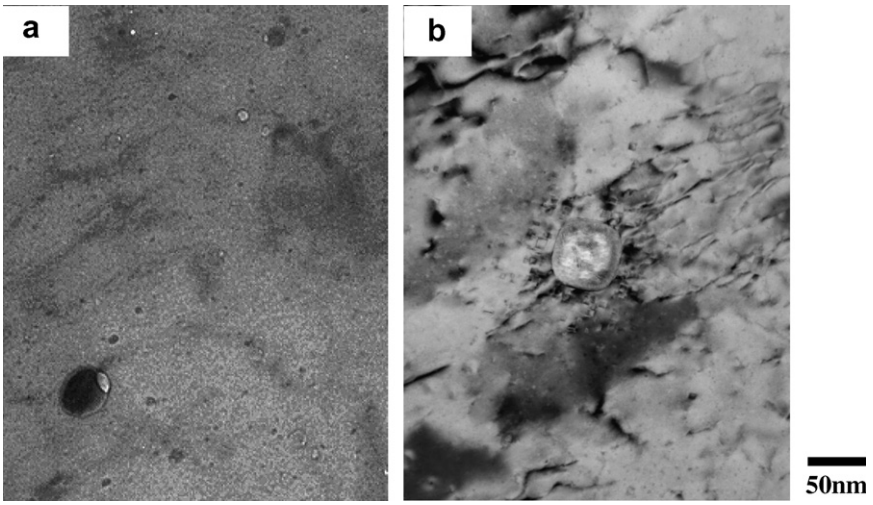

Fig. 2. Bright field TEM micrographs illustrating cavity structure distributed in the matrix. Some cavities were attached at the surface of precipitate; (a) before irradiation, (b) after irradiation at 775 K to 101.0 dpa.

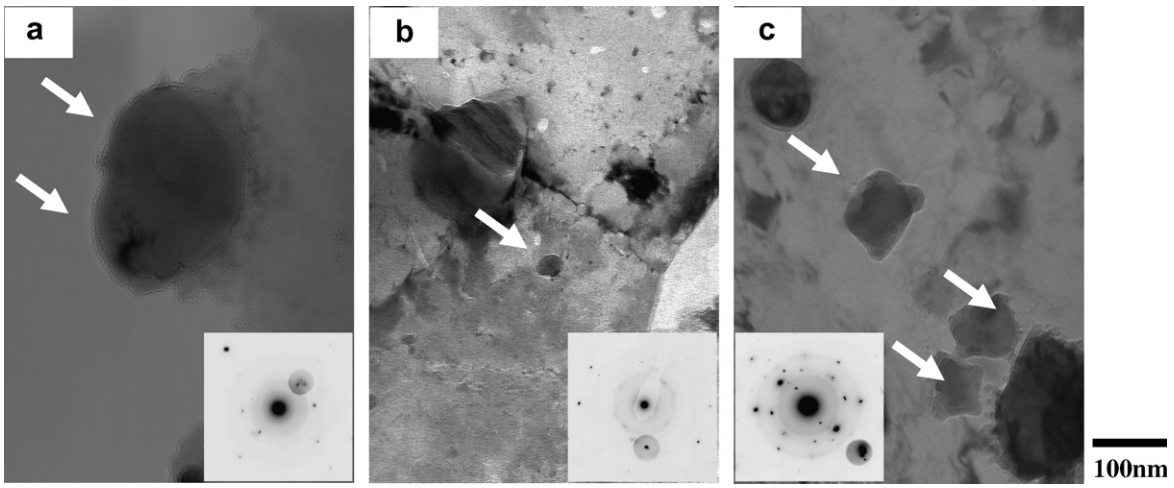

Fig. 3. Bright field TEM micrographs illustrating representative precipitates in MA957 before and after irradiation; precipitates arrowed were (a) Ti oxide, (b) Y–Ti complex oxide and (c) chi-phase (FeCrTiMo). Both (a) and (c) were observed in the sample irradiated at 862 K to 99.0 dpa, whereas (b) was observed in the unirradiated sample.

Table 2
Dispersion parameters of oxide particles measured for the MA957 irradiated to ~100 dpa

		Unirrad.	775 K	982 K
Diameter (nm)	Min.	5.2	9.5	8.7
	Ave.	74.5	84.8	82.0
	Max.	300	186	230
Number density ($\times 10^{13}$ cm^{-3})		2.76	1.16	1.36

near and at the precipitate interfaces and their mean size seemed to grow slightly due to successive irradiations.

In regard to the precipitates, two types of oxide (Ti oxide, Y–Ti complex oxide) and one type of intermetallic compound (chi-phase) were identified by selected area diffraction (SAD) analysis and microchemical analysis. Paired micrographs and the associated SADs are shown in Fig. 3(a)–(c). Y–Ti complex oxide particles were much smaller than Ti oxide particles and the mean size of the former was about one tenth as large as that of the latter. Also, tetragonal-shaped precipitates (Fig. 3(c)) were found to have a cubic structure ($a_0 = \sim 0.92$ nm) and to contain Fe, Cr, Ti and Mo. Both oxides in the unirradiated specimen were found in all the irradiated specimens, but chi-phase was only found in the irradiated specimens.

Dispersion parameters of oxide particles, such as mean size and number density, measured from TEM micrographs are detailed in Table 2. All parameters were average values from arbitrarily selected areas (total area was equal to $5 \times 5\ \mu m^2$) since distribution of oxide particles was relatively uniform and broadly similar despite the anisotropic structure before and after irradiation. Particle size variations were small between unirradiated and irradiated specimens (775, 982 K) though the number densities decreased by about one-half due to irradiation.

4. Discussion

The MA957 has previously been investigated for microstructural evolution under ion irradiation [7], irradiation-induced swelling [8,9], irradiation creep [9,10], mechanical properties [11], and atom probe tomography of oxide dispersoids [12]. Experimental temperatures covered in these reports, however, were limited to below 873 K. The mechanical property degradation of ODS steel planned for use in fusion and fission reactors is closely related to microstructural evolution under irradiation. In most cases, microstructures change when mechanical properties are degraded. In comparison with other structural materials, the benefits of ODS steels are believed to be produced by fine dispersions of thermally stable oxide particles. Therefore, quantitative evaluation of oxide stability under irradiation is quite challenging but essential if desired operating temperatures of future nuclear reactors are to be achieved. It is thus necessary to discuss and anticipate the dynamic interactions between oxide particles and defect structures (e.g. dislocations and cavities) for target operating conditions.

As indicated in Fig. 1(a)–(e), the as-fabricated microstructure of MA957 was highly strained and was not changed macroscopically even at high dose and/or high temperature. Also, irradiation-induced defect clusters such as dislocation loops and newly nucleated cavities were not formed although Ar bubbles were present prior to irradiation and were concentrated near and at the precipitate surfaces (Fig. 2(a)–(c)). These facts are interpreted as follow: the highly strained textures of MA957 contained dense dislocation tangles and networks. This allowed irradiation defects to easily diffuse by many diffusion paths over long distances at elevated temperature and to annihilate at high density sink sites (e.g. grain boundary, dislocation, interface between precipitate and matrix).

Also, the possibility of irradiation-induced changes in existing oxide particles (Fig. 3(a) and (b)) was considered. The present studies implied that all the oxides had uniformly decreased in size by ballistic resolution due to repeated high energy neutron bombardments and also that some tiny oxide particles disappeared. As a result, the number density of fine oxide particles decreased but the average diameter remained nearly unchanged (Table 2). Similar behavior of oxide particles has been reported in European ODS ferritic steel [13]. The chi-phase (Fig. 3(c)) formed during irradiation at elevated temperature was also considered. An aging experiment with the European ODS steel which contained higher Ti and Mo contents than MA957, revealed that chi-phase was thermally precipitated and stable during high temperature aging [2]. Therefore though Mo and Ti contents were lower in MA957, the results show that chi-phase formation was assisted by irradiation at elevated temperature.

Finally, TEM observation revealed that the recoil resolution of oxide might be high. This is a concern, since the benefits of ODS steels were brought about by fine dispersion of thermally stable

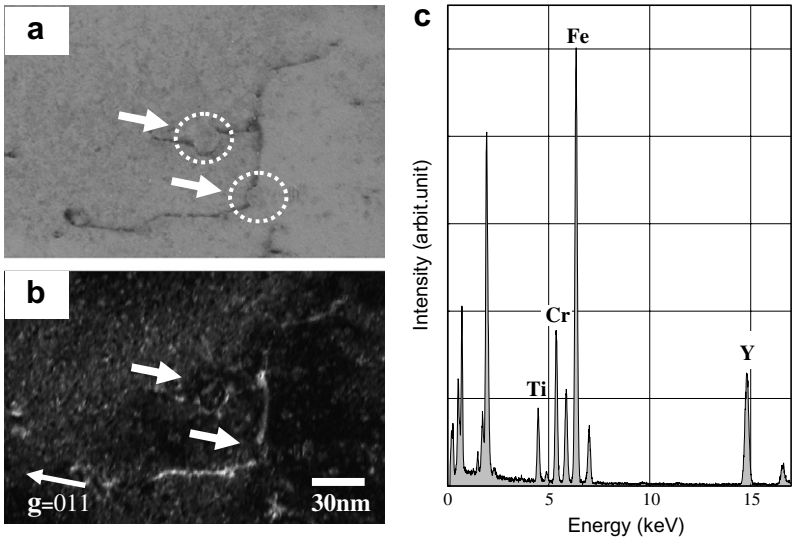

Fig. 4. TEM micrographs and EDS profile exhibiting interaction between fine oxides (arrowed) and dislocation line; (a) bright field image, (b) dark field image taken by using $\mathbf{g} = 011$, and (c) EDS spectrum from fine oxides (arrowed).

oxide particles. On the other hand, a further significant observation specific to the ODS steels was that the relatively fine oxide particles (10–20 nm in diameter) in material irradiated at 982 K to 100.5 dpa have interacted with dislocations during irradiation (Fig. 4(a) and (b)). Fig. 4(c) shows that these oxides particle contained Y and Ti. These results illustrate that as if some oxides particles dissolved under irradiation, surviving oxides particles would still be effective pinning points of dislocations and contribute to sustain the high temperature strength properties. Further consideration on dynamic processes of both solute elements redissolved from oxides is possible during irradiation, based on the fact that neither solute element have high solubility in Fe–Cr–X (X = Y or Ti) ternary system. Namely, Y and/or Ti atoms exceed their solubility limits and would have to segregate or reprecipitate during irradiation unless their solubility limits under irradiation are higher in comparison to their thermally equilibrium systems. In contrast, if their solubility limit became higher during irradiation, solution hardening due to solute elements released from oxides would be expected. Further investigations of oxide particle behavior during irradiation are needed to clarify the dynamic process.

5. Conclusion

Microstructural observation was performed on a ODS ferritic steel (MA957) heavily neutron-irradiated at ~973 K, and the irradiation data base available on ODS steel was extended to this higher temperature. The following conclusions on oxide particles phase stability were obtained:

(1) Diametrical size variations were small between unirradiated and specimens irradiated at 775 and 982 K, though the number densities decreased by about one-half due to irradiation. This implies that the recoil resolution of oxide particles was induced by ballistic bombardment of high energy neutron.
(2) Oxide particles effectively function as pinning points for dislocations even under irradiation to a dose of ~100 dpa at 982 K, demonstrating sustained high temperature strength properties of ODS steels in an irradiation environment.

References

[1] J.J. Huet, L. Coheur, A. De Bremaecker, L. De Wilde, J. Gedopt, W. Hendrix, W. Vandermeulen, Nucl. Technol. 70 (1985) 215.
[2] E.A. Little, in: Effects of Radiation on Materials: 17th International Symposium, ASTM STP 1270 (1996) 739.
[3] S. Ukai, T. Nishida, T. Okuda, T. Yoshitake, J. Nucl. Mater. 258–263 (1998) 1745.
[4] S. Ukai, S. Mizuta, M. Fujiwara, T. Okuda, T. Kobayashi, J. Nucl. Sci. Technol. 39 (7) (2002) 778.
[5] S. Ukai, T. Okuda, M. Fujiwara, T. Kobayashi, S. Mizuta, H. Nakashima, J. Nucl. Sci. Technol. 39 (8) (2002) 872.

[6] S. Yamashita, T. Yoshitake, N. Akasaka, S. Ukai, A. Kimura, Mater. Trans 46 (3) (2005) 493.
[7] K. Asano, Y. Kohno, A. Kohyama, T. Suzuki, H. Kusanagi, J. Nucl. Mater. 155–157 (1988) 928.
[8] D.S. Gelles, J. Nucl. Mater. 233–237 (1996) 293.
[9] M.B. Toloczko, D.S. Gelles, F.A. Garner, R.J. Kurtz, K. Abe, J. Nucl. Mater. 329–333 (2004) 352.
[10] M.B. Toloczko, F.A. Garner, C.R. Eiholzer, J. Nucl. Mater. 258–263 (1998) 1163.
[11] A. Alamo, V. Lambard, X. Averty, M.H. Mathon, J. Nucl. Mater. 329–333 (2004) 333.
[12] M.K. Miller, D.T. Hoelzer, E.A. Kenik, K.F. Russell, J. Nucl. Mater. 329–333 (2004) 338.
[13] P. Dubuisson, R. Schill, M. Hugon, I. Grislin, J. Seran, Effect of Radiation on Materials: 18th International Symposium, ASTM STP 1325 (1999) 882.